

## AN ALTERNATIVE DESCRIPTION OF SWING-BY TRAJECTORIES IN TWO AND THREE DIMENSIONS

**Liliane A. Maia**

Departamento de Matemática, Universidade de Brasília, Brasília-DF  
70910-900, Brazil - E-mail: [lilimaia@unb.br](mailto:lilimaia@unb.br)

**Ricardo R. Fragelli**

Departamento de Engenharia Mecânica, Universidade de Brasília, Brasília-DF  
70910-900, Brazil - E-mail: [fragelli@hotmail.com](mailto:fragelli@hotmail.com)

### ABSTRACT

In this paper we simulate and classify the Swing-by maneuvers of a spacecraft in close approach with a celestial body, alternatively proposing an identification of the category of the orbits in the synodic coordinate system. The mathematical model used is the restricted circular three-body problem in two and three dimensions. In general the classification of orbits are presented in “letter-plots” which consist of graphs of orbital categories represented by letters. The coordinates are chosen from the initial conditions of the problem. In our work we use the periapsis distance  $r_p$  and the spherical angles of the spacecraft. Henceforth, we are able to use spatial rectangular coordinates instead and obtain a view of the spacecraft at its periapsis position and the changes in the trajectory during the close approach. The letters are substituted by points in the new graph where the study of the sign of energy and angular momentum gives the right classification of the orbits.

### INTRODUCTION

The gravity assisted maneuver is a technique used in space missions to reduce fuel consumption like in Weinstein 1992, Swenson 1992, Broucke and Prado 1993, Prado and Broucke 1995 and many others (see Broucke 1988 and reference therein). The standard maneuver uses a close approach with a celestial body to modify the velocity, energy and angular momentum of a dimensionless body (a spacecraft). The model used in the present study is the three-dimensional restricted circular tree-body problem (Szebehely 1967).

For fixed parameters  $V_p$ ,  $r_p$ ,  $\alpha$  and  $\beta$ , to described later, the problem consists of studying the motion of the spacecraft near the close encounter with a secondary body of the system. In particular, the energy and angular momentum of the spacecraft before and after the close approach. Those

quantities are used to classify its orbit up to sixteen classes of orbits, according to the changes in the energy and angular momentum caused by the close encounter (see Prado and Broucke 2000).

The main goal is to simulate a large number of orbits, under some fixed parameters, classify them into those classes and use an alternative model to describe the regions of different classes of orbits.

This alternative description of orbital regions, differently from the standard ones found in the literature, uses the spatial rectangular coordinates in the rotating reference system. Henceforth, it is possible to obtain a view of the spacecraft at its periapsis position together with its class of orbit. Moreover, using this alternative model it is possible to derive equations in order to obtain necessary conditions for similarity between two systems.

## MATHEMATICAL MODEL

For the present study the well known model of three-dimensional restricted circular three-body problem (Szebehely 1967) is used. It consists of two bodies  $M_1$  and  $M_2$ , called primaries, of masses  $m_1$  and  $m_2$  moving in circular orbits about their mutual center of mass, with constant angular velocity  $\omega$ , and a third body  $M_3$  of negligible mass (the spacecraft) which moves under the gravitational effect of the central and perturbing masses without affecting their motion. As usual, dimensionless units are used, in such way that the distance between the primaries, the total mass of the system and the angular velocity  $\omega$  of the system are equal to one. The equations of motion of the third body in the rotating frame are given by

$$\left\{ \begin{array}{l} \ddot{x} - 2\dot{y} = x - (1-\mu) \frac{x+\mu}{r_1^3} - \mu \frac{x-(1-\mu)}{r_2^3} \\ \ddot{y} + 2\dot{x} = y - (1-\mu) \frac{y}{r_1^3} - \mu \frac{y}{r_2^3} \\ \ddot{z} = -(1-\mu) \frac{z}{r_1^3} - \mu \frac{z}{r_2^3} \end{array} \right.$$

where  $\mu = \frac{m_2}{m_1 + m_2}$ ,  $r_1$  and  $r_2$  are the distances from  $M_1$  and  $M_2$  to  $M_3$ , respectively. In the case of planar motion  $z = 0$ . It is also necessary to have equations to calculate the energy ( $E$ ) and angular momentum ( $C$ ) of the spacecraft, which are respectively the following

$$E = \frac{(x + \dot{y})^2 + (\dot{x} + y)^2}{2} - \frac{1-\mu}{r_1} + \frac{\mu}{r_2} \text{ and } C = x^2 + y^2 + xy - \dot{x}y.$$

In the restricted problem neither the orbital energy nor the angular momentum are conserved since the third body does not affect the motion of the primaries. However, the dynamical system still has na

integral of the motion, the Jacobi constant, given by  $J = \frac{1}{2}V^2 - \Omega$ , where  $\Omega = \frac{1}{2}(x^2 + y^2) + \frac{1-\mu}{r_1} + \frac{\mu}{r_2}$ .

### ALGORITHM TO SOLVE THE PROBLEM

In order to describe the maneuver it is standard to use the four independent parameters:

- i)  $V_p$ , the magnitude of the velocity of the spacecraft at periapsis; for our purposely velocity vectors  $\vec{V}_p$  parallel to the  $x$ - $y$  plane were considered;
- ii)  $r_p$ , the distance between the spacecraft and the second mass  $M_2$  during the closest approach (periapsis);
- iii)  $\alpha$ , the angle between the projection of the periapsis line in the  $x$ - $y$  plane and the line that connects the two primaries;
- iv)  $\beta$ , the elevation angle between the periapsis line and the  $x$ - $y$  plane.

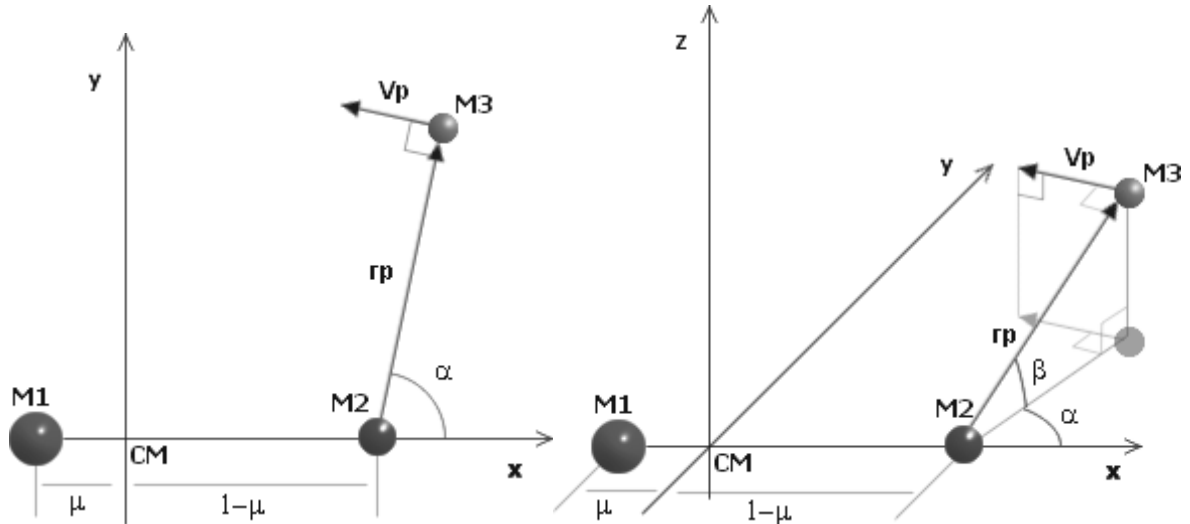


Figure 1 – Initial conditions in two and three-dimensions.

Once a system is established (i.e.,  $\mu$  is fixed at some value), the initial position  $(x_i, y_i, z_i)$  and velocity  $(V_{x_i}, V_{y_i}, V_{z_i})$  are considered for the spacecraft at periapsis. With these considerations, a numerical algorithm is built using MapleV software to solve the problem, in the following steps:

- i) arbitrary values for the parameters  $V_p$ ,  $r_p$ ,  $\alpha$  and  $\beta$  are given;
- ii) with these values, the initial conditions in the rotating system are computed  

$$x_i = (1 - \mu) + r_p \cos \beta \cos \alpha \quad y_i = r_p \cos \beta \sin \alpha \quad z_i = r_p \sin \beta$$

$$V_{x_i} = -V_p \sin \alpha \quad V_{y_i} = V_p \cos \alpha \quad V_{z_i} = 0$$
- iii) with these initial conditions, the equations of motion are integrated forward in time until the distance  $r_2$  is equal to 0.5, half the distance between the primaries in the dimensionless

- system. At this point the numerical integration is stopped and the energy ( $E +$ ) and the angular momentum ( $C +$ ) after the close encounter are calculated;
- iv) the initial conditions are considered again and the equations of motion are integrated backwards in time, until the specified distance is reached again. Then the energy ( $E -$ ) and angular momentum ( $C -$ ) before the encounter are obtained.

For all simulations, a Runge-Kutta 4<sup>th</sup>-5<sup>th</sup> order was used, performed by MapleV software. The energy determines whether the trajectory is elliptic ( $E < 0$ ) or hyperbolic ( $E > 0$ ) and the angular momentum indicates when it is retrograde ( $C < 0$ ) or direct ( $C > 0$ ). Parabolic trajectories are given by  $E = 0$  and linear trajectories by  $C = 0$ . The goal is to identify the category of the orbit of the spacecraft before and after the close encounter for a large range of given initial conditions. The standard classification and representation according to the change in the orbit of the spacecraft is by assigning letters to orbits, the so called “letter-plot” diagram forend in the related literature (Broucke 1988). In the planar case, letter-plots are represented in two-dimensional diagrams that have  $\alpha$  in the horizontal axis and the Jacobi constant  $J$  in the vertical axis, for fixed values of  $r_p$  and  $\mu$ . In the three-dimensional restricted circular three-body problem, a letter-plot is made for fixed values of  $r_p$ ,  $\mu$  and  $V_p$ , in a diagram that has angle  $\alpha$  in the vertical axis and angle  $\beta$  in the horizontal axis (see Felipe 2000).

## RESULTS

In this study a velocity at periapsis  $V_p$  is fixed and the  $r_p$  is a variable taking values in an interval where the influence of  $M_2$  in the change of orbit of the spacecraft is significant. The value of  $r_p$  should not be so large such that the gravitational force of  $M_2$  on the spacecraft would hardly be noticed, neither it should not be so small to result in capture of the spacecraft for a long period.

According to Broucke 1988, where a convenient interval for the Jacobi constant  $J$  is assumed  $-1.45 \leq J \leq 1.5$ , it is necessary to find the corresponding  $V_p$ ’s for  $J$  in this interval.

The Earth-moon system ( $\mu = 0.01$ ) is initially fixed and for  $r_p$ ’s found in Broucke 1998, it is possible to obtain lower and upper bounds for  $V_p$ ’s corresponding to  $-1.45 \leq J \leq 1.5$ .

Table 1 – Ranges for  $V_p$ ’s corresponding to  $-1.45 \leq J \leq 1.5$ .

$r_p$	Lower $V_p$	Upper $V_p$
0.01	1.435407970	2.821417381
0.001	4.478850632	5.095105787
0.0001	14.14426032	14.35131004

In order to perform the simulations of orbits, the values chosen for  $V_p$ ’s are 1.5, 2, 2.5, 3, 4, 5, 10 and 14.

Considering  $J$  constant with respect to the angle  $\alpha$ , it is possible to calculate lower and upper bounds for  $r_p$ 's for each  $V_p$  fixed, as it is shown in table 2.

Note that for each  $V_p$  fixed it is possible to find an  $r_p$  such that the calculated  $J$  is equal to  $-1.45$ , however the same does not happen for  $J = 1.5$ . In the latter cases, or in case the calculated upper bound for  $r_p$  is superior to the radius of influence, it is taken the upper bound  $r_p = 0.04$  for the study of orbital regions.

Table 2 – Initial conditions for the study of orbital regions.

$V_p$	<b>Lower <math>r_p</math> calculated</b>	<b>Upper <math>r_p</math> calculated</b>	<b>Lower <math>r_p</math> assumed</b>	<b>Upper <math>r_p</math> assumed</b>
1.5	0.0091339	Não tem	0.009	0.04
2.0	0.005076	Não tem	0.005	0.04
2.5	0.0032311	0.07277	0.0032	0.04
3.0	0.00223717	0.00657944	0.002237	0.0066
4.0	0.00125471	0.00199205	0.00125	0.002
5.0	0.000801928	0.00105043	0.0008	0.0011
10.0	0.000200120	0.000212676	0.0002	0.00022
14.0	0.000102072	0.000105241	0.000102	0.00011

With  $\mu = 0.01$  and  $V_p$  fixed for a value in table 2, a simulation of an orbit is performed for each initial condition as defined before, for  $r_p$  in that interval and the orbit is classified according to the signs of  $E -$ ,  $E +$ ,  $C -$  and  $C +$ .

An example of the results obtained and represented in this alternative diagram is shown below for  $V_p = 1.5$ .

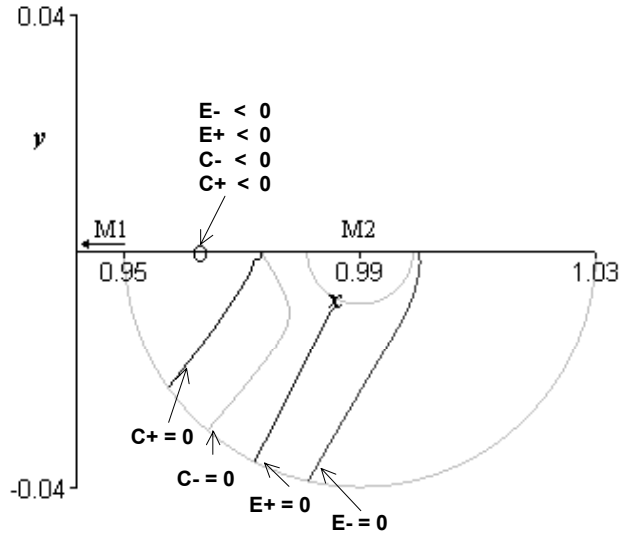


Figure 2 – Orbital regions for  $V_p = 1.5$  and  $0.009 \leq r_p \leq 0.04$  in Earth-moon system.

In order to understand this representation, consider two points  $P_1$  and  $P_2$  which are indicated in the diagrams as initial conditions. The point  $P_1$  has polar coordinates  $\alpha = 232^\circ$  and  $r_p = 0.03$  and  $P_2$  has  $\alpha = 300^\circ$  and  $r_p = 0.03$ .  $P_1$  is found in a region of type A (direct ellipse to direct ellipse) and  $P_2$  is located in a region K (direct hyperbola to direct hyperbola).

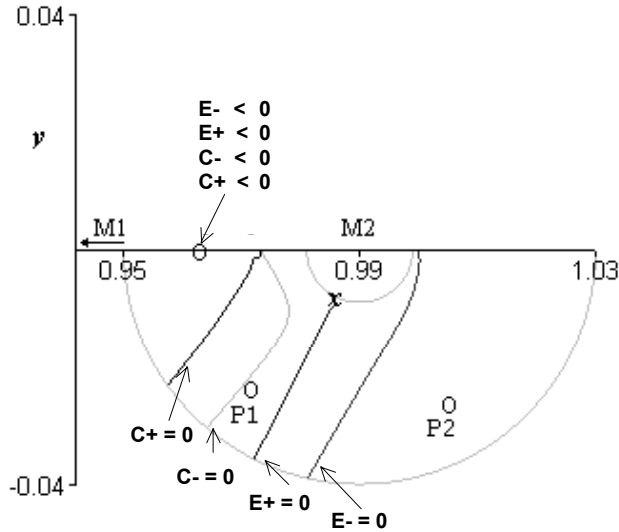


Figure 3 – Representation of points  $P_1$  and  $P_2$  in diagram of orbital regions.

A simulation of the trajectories of the spacecraft in the rotating reference system, under the fixed parameters  $\mu = 0.01$ ,  $V_p = 1.5$  and periapsis at  $P_1$  and  $P_2$  is shown in figure 5.



Figure 4 - Trajectories of the spacecraft in regions A and K for a short time.

Note that for a longer period, one trajectory is a spiral around the center of mass, characteristic of a hyperbolic orbit, and the other is a trajectory composed of small loops enclosing the bigger primary, which characterizes an elliptic orbit.

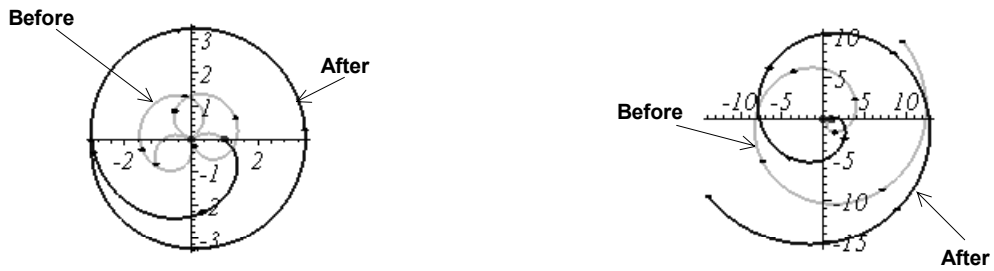


Figure 5 - Trajectories of the spacecraft in regions A and K for a long time.

Simulations for other values of the parameter  $V_p$  in table 2 give the following diagrams of orbital regions.

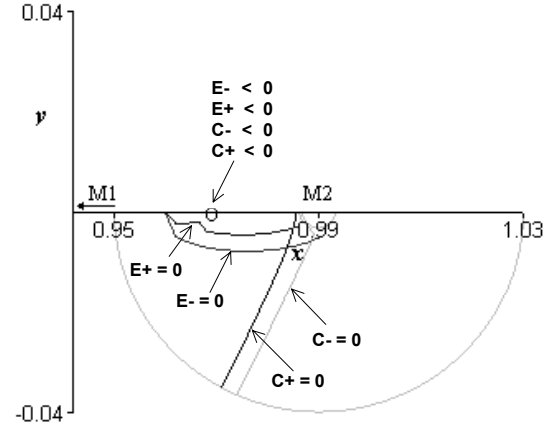
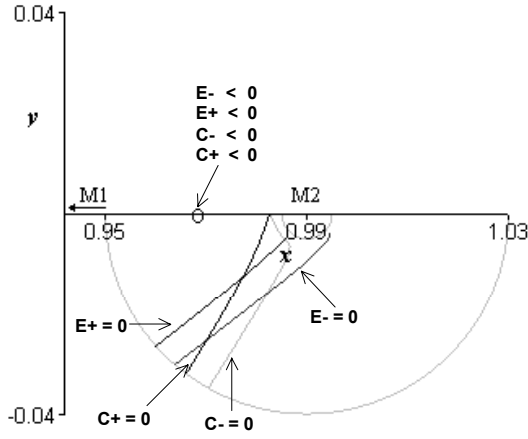


Figure 6 - Orbital regions for  $V_p = 2$  and  $0.005 \leq r_p \leq 0.04$  (left) and for  $V_p = 2.5$  and  $0.0032 \leq r_p \leq 0.04$  (right).

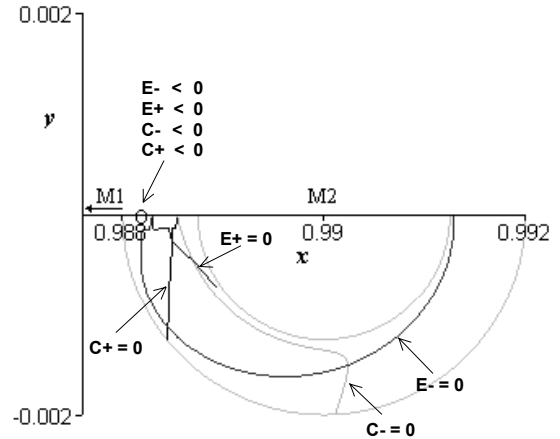
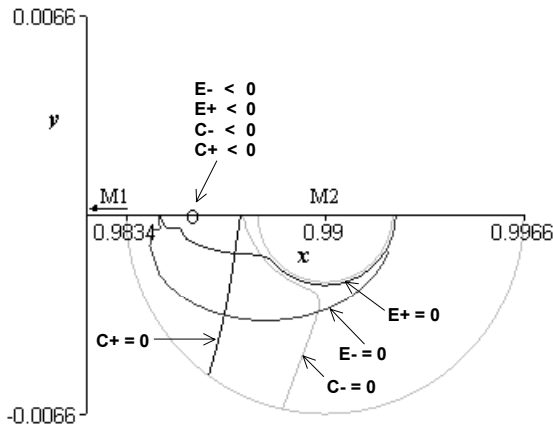


Figure 7 - Orbital regions for  $V_p = 3$  and  $0.002237 \leq r_p \leq 0.0066$  (left) and for  $V_p = 4$  and  $0.00125 \leq r_p \leq 0.002$  (right).

In each graph a point on the axis of the primaries indicates the signs of the functions  $E-$ ,  $E+$ ,  $C-$ ,  $C+$  at that point. As one moves to the right hand side and crosses their zero level curves, then the signs of these functions change from negative into positive at points chosen in the ring domain.

Note that the zero level curves of the energy ( $E- = 0$  and  $E+ = 0$ ) look alike and are almost parallel for  $V_p$  small. When they intercept the horizontal axis they meet at  $\alpha = 180^\circ$  and  $\alpha = 360^\circ$ . Similarly for the zero level curves of the angular momentum ( $C- = 0$  e  $C+ = 0$ ) which leave the ring domain for larger radii almost at  $\alpha = 270^\circ$ . If  $V_p > 2$  and  $r_p$ 's are sufficiently large the energies ( $E-$  and  $E+$ ) are positive and the regions are reduced to three classes (retrograde hyperbola to retrograde hyperbola, retrograde hyperbola to direct hyperbola and direct hyperbola to direct hyperbola). Moreover, those regions are delimited by curves of zero angular momentum. As  $r_p$  increases, those curves approach asymptotically a line at M2 of constant angle  $\alpha$ , which for  $C+$  is close to  $\alpha = 270^\circ$ .



## SIMILARITY RESULTS

The objective now is to develop a technique that may permit associating two systems which have similar diagrams of orbital regions, under different parameters and initial conditions.

Broucke in (Broucke 1988) verified that letter-plot diagrams of orbital regions, in the coordinate system of variables  $\alpha$  and  $J$  in the axis, are similar for given parameters  $\mu = C_1$  and  $r_p = C_2 \cdot C_1$ , if pairs of values are taken in the sets  $C_1 = 0.01, 0.001, 0.0001$  and  $0.00001$  and  $C_2 = 0.01, 0.1, 1, 10, 100$ . In fact, if there is similarity of diagrams then

$$r_{p2} = r_{p1} \frac{\mu_2}{\mu_1}, \quad (1)$$

where  $(r_{p1}, \mu_1)$  and  $(r_{p2}, \mu_2)$  are periapsis radii and the coefficients of mass for systems 1 and 2, respectively.

Once  $\mu = 0.01$ ,  $r_p = 0.01$  and  $\alpha = 180^\circ$  are fixed, the velocities  $V_p$  are calculated corresponding to  $-1.5 \leq J \leq 1.5$ , and the values obtained are  $1.400141436 \leq V_p \leq 2.821417381$ . Then, a value of  $V_p$  is fixed and the dependence of  $J$  with respect to the independent variable  $\alpha$  can be measured.

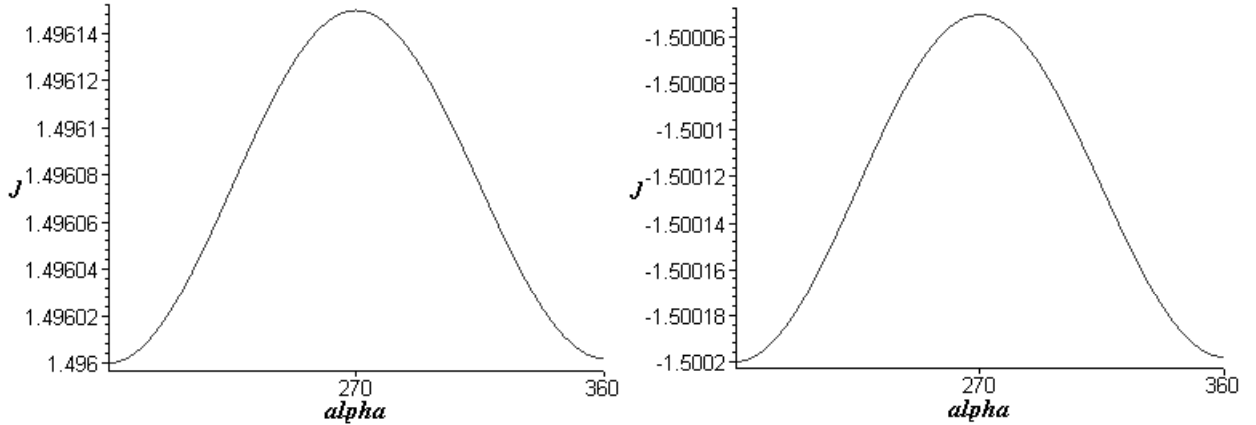


Figure 8 - Relation between the Jacobi constant and  $\alpha$  for fixed  $V_p$  and  $r_p$ .

The Jacobi constant  $J$  may be considered a constant function of the variable angle  $\alpha$ , with an error smaller than  $10^{-4}$ , for  $r_p = 0.01$ . It is assumed that the initial conditions  $\mu = 0.01$ ,  $r_p = 0.01$  and  $-1.5 \leq J \leq 1.5$  may be replaced by  $\mu = 0.01$ ,  $r_p = 0.01$  and  $1.400141436 \leq V_p \leq 2.821417381$ , giving the same diagrams of orbital regions. Analogously, for  $\mu = 0.001$  and  $r_p = 0.001$ , again assuming  $J$  constant with respect to  $\alpha$ , the corresponding velocity values are

$1.412800055 \leq V_p \leq 2.827720636$ , and so on. The following table shows the same calculations for other pairs  $(\mu, r_p)$ .

Table 3 - Ranges of velocities corresponding to $-1.5 \leq J \leq 1.5$	
Initial Conditions	Calculated Interval of Velocities
$(\mu = 0.01, r_p = 0.01)$	$1.400141436 \leq V_p \leq 2.821417381$
$(\mu = 0.001, r_p = 0.001)$	$1.412800055 \leq V_p \leq 2.827720636$
$(\mu = 0.0001, r_p = 0.0001)$	$1.414072148 \leq V_p \leq 2.828356420$
$(\mu = 0.00001, r_p = 0.00001)$	$1.414199420 \leq V_p \leq 2.828420054$

These pairs of initial conditions are equivalent in the sense that for the corresponding intervals of velocities  $V_p$  's their diagrams of orbital regions should be similar.

Now, fixing  $V_p = 2.821417381$  (case  $\mu = 0.01$ ) and calculating an interval of  $r_p$  's such that  $J$  takes its standard values, it results in  $0.002499913301 \leq r_p \leq 0.01$ . Analogously, if  $V_p = 2.827720636$  (case  $\mu = 0.001$ ) then the resulting interval of  $r_p$  's is  $0.0002499999122 \leq r_p \leq 0.01$ .

Therefore,  $V_p = 2.821417381$  ( $\mu = 0.01, r_p = 0.01$ ) is equivalent to  $V_p = 2.827720636$  ( $\mu = 0.001, r_p = 0.001$ ) and both represent a horizontal line in the diagrams of orbits in coordinates  $J, \alpha$ . Other simulations for those initial conditions and other choices of  $r_p$  's show a similarity between these two systems.

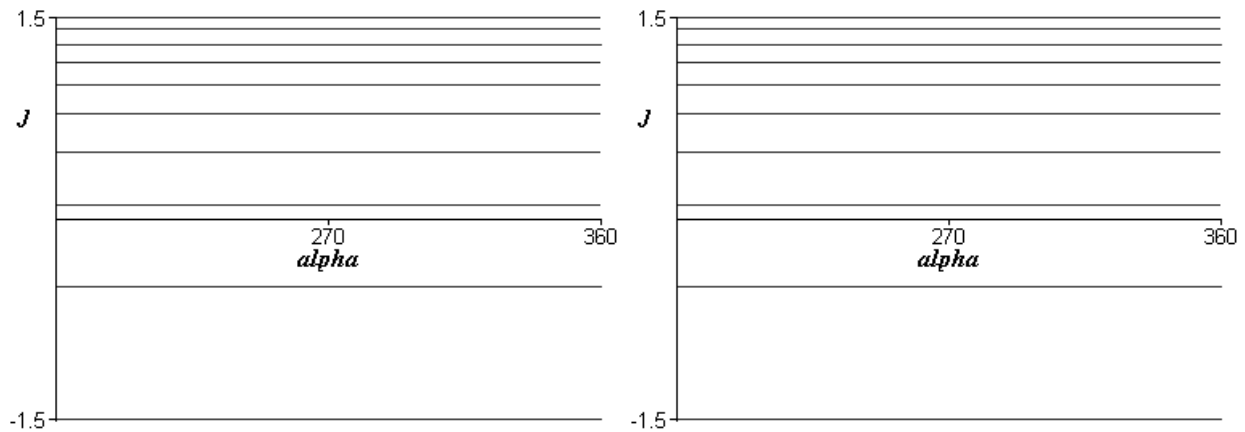


Figure 9 - Study of  $J$  for different values of  $r_p$  in two systems

However, for lower velocities like  $V_p = 1.400141436$  ( $\mu = 0.01$ ) it is not possible to find an interval of  $r_p$  's which would give the standard interval of  $J$  's. Moreover, here  $J$  is not a constant function of the variable  $\alpha$ , as the following examples show. The left hand side shows from top to bottom the

cases  $\mu = 0.01$  and  $r_p$  varying in the intervals  $[0.01, 0.2]$  and  $[0.01, 0.5]$ , and the right hand side shows in the same order, cases  $\mu = 0.001$  and  $r_p$  taking values in the intervals  $[0.001, 0.02]$  and  $[0.001, 0.05]$ .

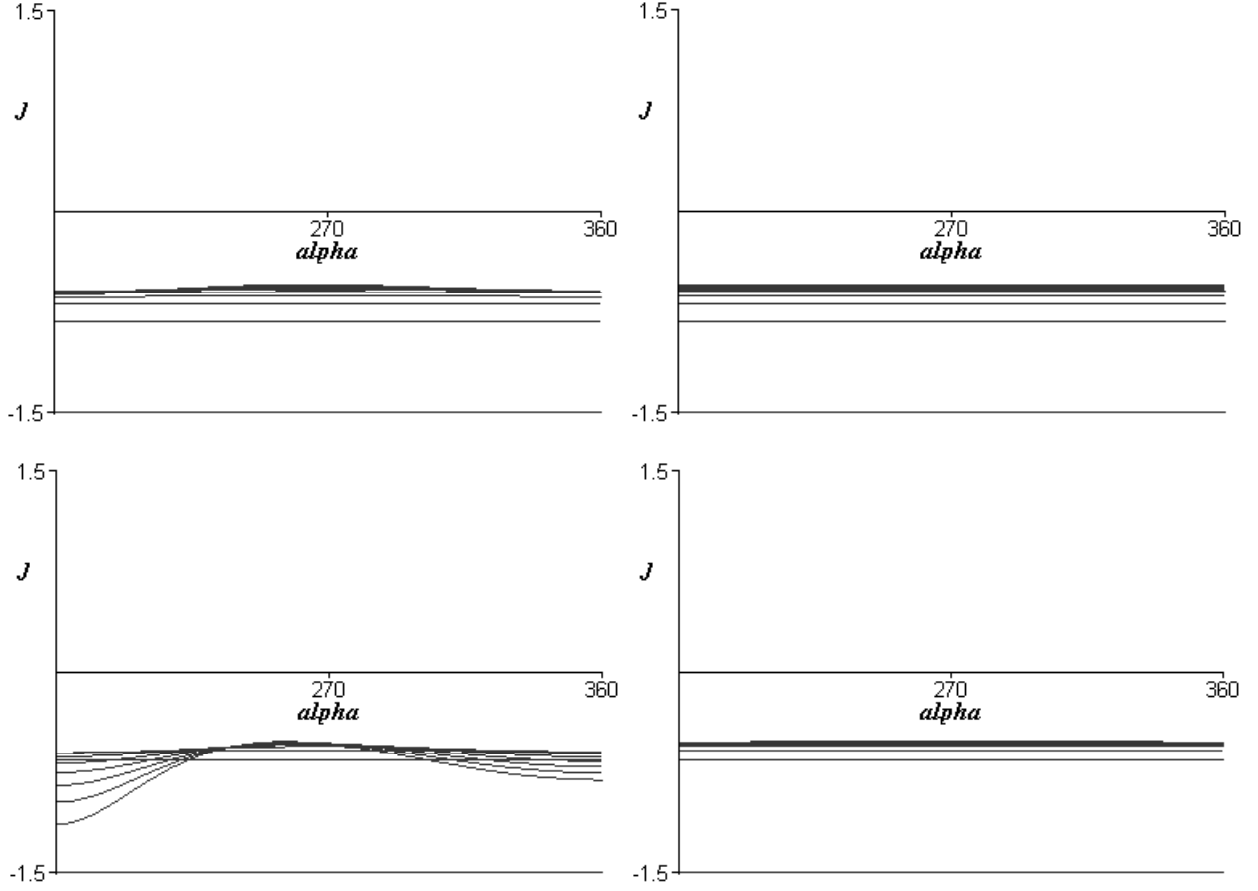


Figure 10 - Study of  $J$  for different intervals of  $r_p$  in two systems

Given two systems with periapsis  $r_{p1}$  and  $r_{p2}$  and coefficients of mass  $\mu_1$  and  $\mu_2$ , respectively, for the purpose of this study if there is similarity then equation (1) is satisfied. This implies that if  $r_{p1}$  is taken equal to  $\mu_1$  then  $r_{p2}$  is equal to  $\mu_2$ . Moreover, if their Jacobi constants  $J_1$  and  $J_2$  are assumed constant functions of the angle  $\alpha$ , then  $\alpha$  may be taken equal  $180^\circ$ . With these initial conditions, in order to obtain similarity it is assumed  $J_1 = J_2$  and it follows that their respective periapses velocities  $V_{p1}$  and  $V_{p2}$  in the rotational reference system must satisfy the condition:

$$V_{p2} = \sqrt{V_{p1}^2 - (1 - 2\mu_1)^2 + (1 - 2\mu_2)^2}. \quad (2)$$

Some examples of similar diagrams of orbital regions are given below for high and low velocities. Their respective initial conditions satisfy equations (1) and (2).

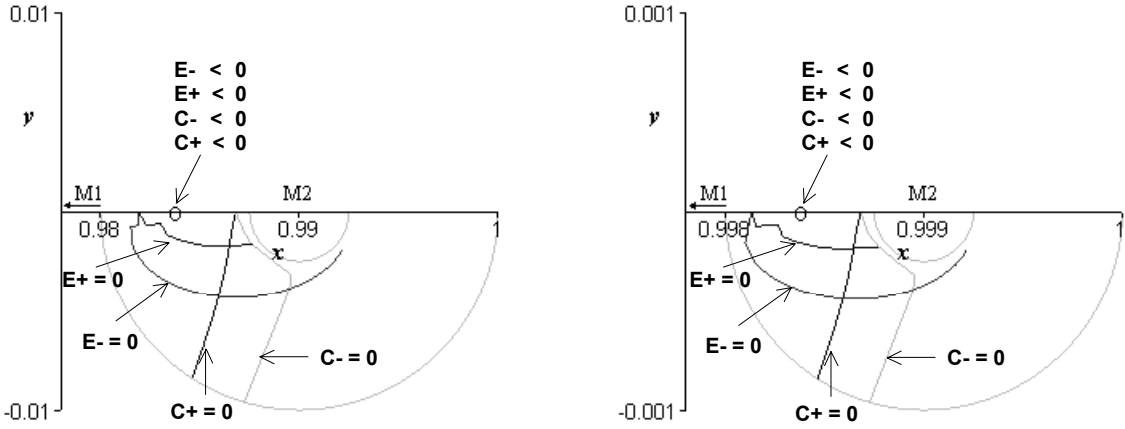


Figure 11 - Similar diagrams of orbital regions for two different systems  $V_{p1} = 2.82142$  and  $\mu_1 = 0.01$  (left) and  $V_{p2} = 2.82772$  and  $\mu_2 = 0.001$  (right).

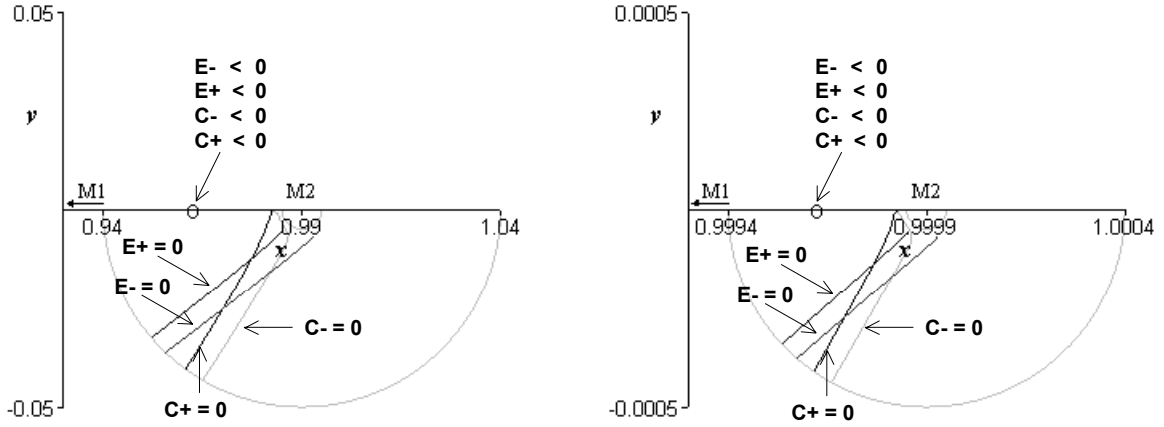


Figure 12 - Similar diagrams of orbital regions for two different systems  $V_{p1} = 2.0$  and  $\mu_1 = 0.01$  (left) and  $V_{p2} = 2.00978$  and  $\mu_2 = 0.0001$  (right).

### ORBITAL REGIONS IN THREE DIMENSIONS

The study of three-dimensional orbital regions involves one more variable: the angle  $\beta$ . Simulations are performed for a spherical shell taking  $V_p$  fixed and  $0 \leq \beta \leq 90^\circ$ , since there is symmetry for  $-90^\circ \leq \beta \leq 0$ . Each of the sixteen classes of regions is viewed separately. For a fixed angle  $\beta$ , the points of the boundary of a region are determined. Then, the angle  $\beta$  takes different values between 0 and 90 in order to generate different surfaces. Finally, these surfaces are put together in order to generate the desired region.

A better view of a region is obtained using MapleV to produce animations of the three-dimensional picture. The following pictures illustrate the type of view obtained as output of the programs for  $V_p = 1.5$ .

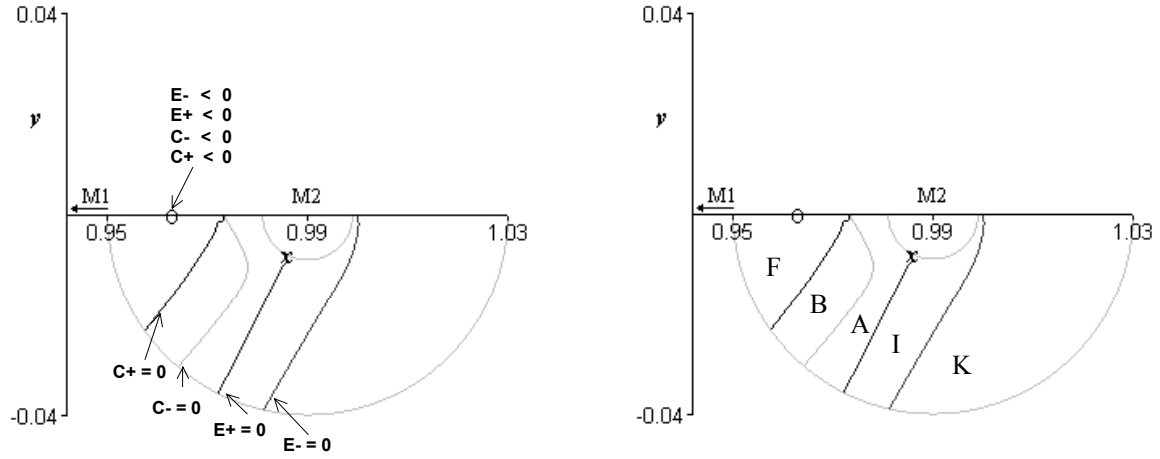


Figure 13 - Orbital regions for  $V_p = 1.5$  including the letters of classes of orbits.

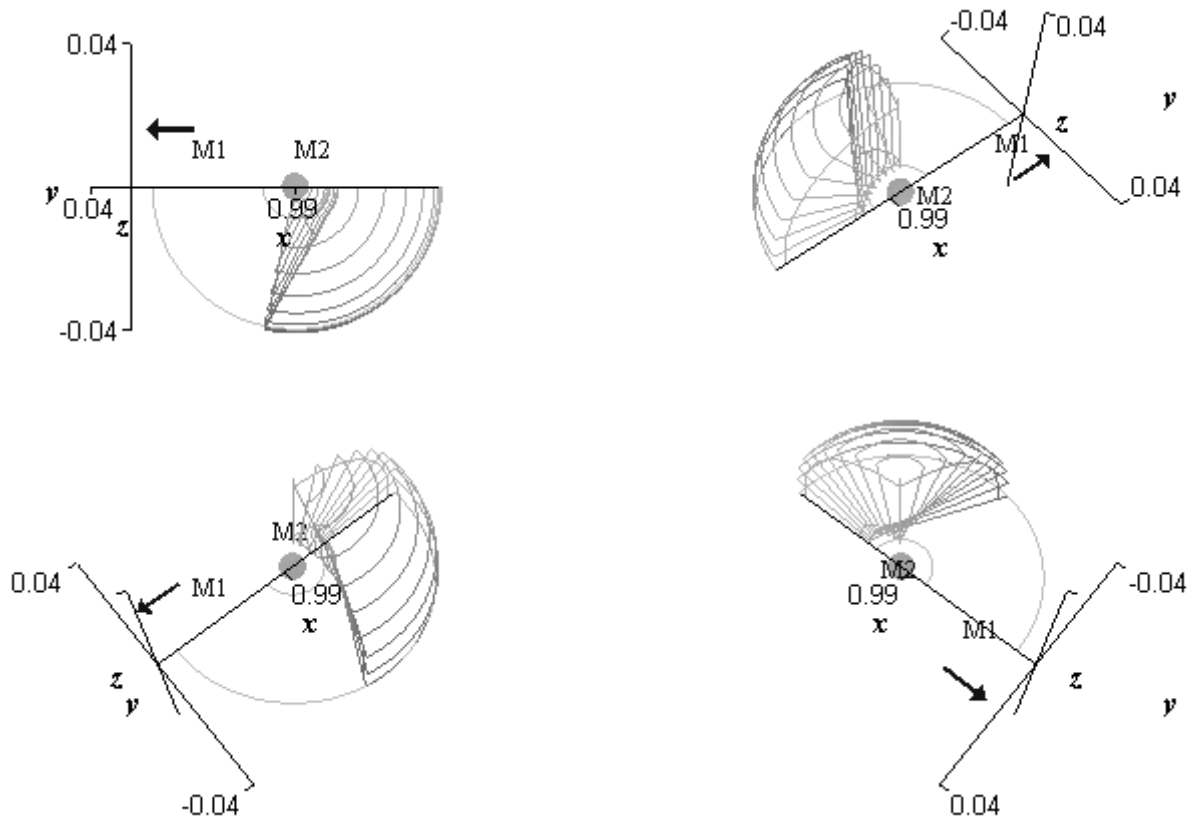


Figure 14 - Region K (direct hyperbola to direct hyperbola).

## CONCLUSIONS

The effects of a close approach of a spacecraft with a celestial body were simulated and classified, using a numerical algorithm and the plotting resources of MapleV software. An alternative description of diagrams of orbital regions in the rotational coordinate system is proposed. The

mathematical model used is the restricted circular three-body problem in two and three dimensions. In general the classification of orbits are presented in “letter-plots” which consist of graphs of orbital categories represented by letters. In this work the periapsis distance  $r_p$  and the spherical angles  $\alpha$  and  $\beta$  of the spacecraft are used as variables, and the periapsis velocity  $V_p$  is fixed. Henceforth, it is possible to use spatial rectangular coordinates instead and obtain a view of the spacecraft at its periapsis position and a classification of the changes in the trajectory during the close approach, simultaneously at the same diagram.

Moreover, a procedure was developed to study the similarity of two systems, or equivalently, the similarity of two diagrams of orbital regions for different initial conditions. Equations involving the periapsis radii, the coefficients of mass and the velocities of two systems, were derived as necessary conditions for similarity of two systems.

## REFERENCES

- BROUCKE, R.A.**; *The celestial mechanics of gravity assist*. AIAA/AAS Astrodynamics Conference, Minneapolis, MN, **1988** (AIAA Paper 88-4220).
- BROUCKE, R.A. & A.F.B.A. PRADO** (1993). "Jupiter Swing-By Trajectories Passing Near the Earth", *Advances in the Astronautical Sciences*, Vol. 82, No 2, pp. 1159-1176.
- BROUCKE, R.A.; PRADO, A.F.B.A.**; *A study of the effects of jupiter in space trajectories*. IX Colóquio Brasileiro de Dinâmica Orbital, **2000**.
- FARQUHAR, R.W. & D.W. DUNHAM** (1981). "A New Trajectory Concept for Exploring the Earth's Geomagnetic ", *Journal of Guidance, Control and Dynamics*, Vol. 4, No. 2, pp. 192-196.
- FELIPE, G.; PRADO, A.F.B.A.**; *Optimal maneuvers in three dimensional swing-by trajectories*. IX Colóquio Brasileiro de Dinâmica Orbital, **2000**.
- FRAGELLI, R. R.**; *Estudo da manobra assistida pela gravidade em duas e três dimensões*, Tese de mestrado, Departamento de Engenharia Mecânica, Universidade de Brasília, **2002**.
- FRAGELLI, R. R.; MAIA, L. A.**; *The powered swingby in three dimensions*. X Colóquio Brasileiro de Dinâmica Orbital, Guaratinguetá, **2000**.
- PRADO, A.F.B.A. & R.A. BROUCKE** (1995). "A Classification of Swing-By Trajectories using The Moon". *Applied Mechanics Reviews*, Vol. 48, No. 11, Part 2, November, pp. 138-142.
- PRADO, A.F.B.A.**; *An analytical description of the close approach maneuver in three dimensions*. IAF-00-A5.05, **2000**.
- SZEBEHELY, V.**; *Theory of orbits*, Academic Press, New York, **1967**.
- SWENSON, B.L.** (1992). "Neptune Atmospheric Probe Mission", AIAA Paper 92-4371.
- WEINSTEIN, S.S.** (1992). "Pluto Flyby Mission Design Concepts for Very Small and Moderate Spacecraft", AIAA Paper 92-4372.